ARTICLES

Competing Pathways in the Infrared Multiphoton Dissociation of Hexafluoropropene

C. A. Longfellow, L. A. Smoliar, and Y. T. Lee*

Chemical Sciences Division, Lawrence Berkeley Laboratory and Department of Chemistry, University of California, Berkeley, California 94720

Y. R. Lee, C. Y. Yeh, and S. M. Lin

Institute of Atomic and Molecular Sciences, Academia Sinica, P.O. Box 23-166, Taipei, Taiwan

Received: February 29, 1996[⊗]

The infrared multiphoton dissociation of hexafluoropropene was studied by photofragment translational spectroscopy. Two primary channels and one secondary channel were identified. The predominant primary channel produces CF_3CF or C_2F_4 and CF_2, with the heavier species undergoing further dissociation to two CF_2 fragments. A number of dissociation mechanisms are proposed for the elimination of CF_2, including direct cleavage of the carbon−carbon double bond. In the second primary channel, a simple bond rupture reaction produces CF_3 and C_2F_3. As expected, the translational energy distribution for this channel peaks near zero, indicating no exit barrier is present. The activation energy for this simple bond rupture is estimated to be 100−105 kcal/mol. The branching ratio, $[CF_2]/[CF_3]$, between the two primary pathways is 4.0 ± 1.0.

I. Introduction

The decomposition of hexafluoropropene has been previously investigated using both thermal and infrared multiphoton dissociation (IRMPD) techniques. A single primary reaction (1) was proposed on the basis of a thermal decomposition experiment, although neither of the products, tetrafluoroethylene or difluorocarbene, was directly observed.[1]

$$C_3F_6 \rightarrow C_2F_4 + CF_2 \quad (1)$$

An activation energy of 75 kcal/mol was estimated for reaction 1; however, because of the circuitous method used to obtain this value, it is listed as highly questionable in a compilation of gas kinetic data.[2] In a later investigation, perfluoroisobutene, perfluoro-1-butene, and perfluoro-2-butene were identified as pyrolysis products of hexafluoropropene, highlighting the extensive role of recombination in this reaction.[3]

In a more recent study, a free-piston adiabatic compression setup was used to decompose hexafluoropropene.[4] In the initial compression stages the only product identified was tetrafluoroethylene, and an activation energy of 82.7 ± 1 kcal/mol was obtained for reaction 1. From their experiment Buravtsev et al. predict that the precursor to tetrafluoroethylene (C_2F_4) is trifluoromethylfluorocarbene (CF_3CF), which initially forms in the dissociation of hexafluoropropene (2).

$$C_3F_6 \rightarrow CF_3CF + CF_2 \quad (2)$$

A subsequent 1,2-fluorine atom shift (reaction 3) was suggested to take place without a barrier, with the carbene species 17 ± 1.5 kcal/mol higher in energy than tetrafluoroethylene.

$$CF_3CF \rightarrow C_2F_4 \quad (3)$$

Reaction 3 has also been suggested in mercury-sensitized photolysis[5] and flash photolysis[6] studies of hexafluoropropene. Nevertheless, the prediction of a barrierless reaction from the adiabatic compression studies is somewhat surprising as experimental[7] and theoretical[8] studies on fluorine atom shifts in CF_3CH have found barriers greater than 20 kcal/mol.

With the widespread availability of high-power CO_2 lasers, IRMPD studies have become a practical alternative to thermal studies. The possibility of exciting the C−F stretch on the central carbon of hexafluoropropene at 1037 cm^{-1} makes this compound a viable candidate for such infrared multiphoton pumping.[9,10] In a previous IRMPD experiment, the products C_2F_4 and C_2F_6 were identified.[10] The production of C_2F_4 is postulated to result from reaction 1 as well as from the recombination of CF_2 radicals. One possible mechanism used to explain the presence of C_2F_6 is a fluorine abstraction, reaction 4, followed by recombination (5).

$$CF_2 + CF_2 \rightarrow CF_3 + CF \quad (4)$$

$$CF_3 + CF_3 \rightarrow C_2F_6 \quad (5)$$

In another IRMPD study, the major products, C_2F_4 and C_2F_6, were identified by their infrared absorption spectra.[11] The fluence dependence of the yield of the products was further probed as discussed in a subsequent paper.[12] Higher fluence favors formation of C_2F_6, but with prolonged irradiation C_2F_6 and C_2F_4 production decreases. The authors suggested that reactions 1, 4, and 5 cannot completely describe the hexafluoropropene dissociation mechanism. Upon further examination of the infrared spectra, absorption lines attributable to poly(tetrafluoroethylene) were identified. It is hypothesized that the incorporation of CF into poly(tetrafluoroethylene) ($-CF_2-CF_2$) does not change the absorption spectra significantly and can explain the eventual fate of the CF radicals from reaction 4.

As indicated by the experiments carried out so far, the results of the decomposition experiments of hexafluoropropene are

* To whom correspondence should be addressed.
⊗ Abstract published in *Advance ACS Abstracts,* December 15, 1996.

S1089-5639(96)00653-6 CCC: $14.00

difficult to interpret. This is because of the multiple collisions that take place after the initial unimolecular decomposition, obscuring the primary decomposition pathways. Besides the primary reactions already discussed (1, 2), rupture of the carbon−carbon single bond may be possible (6).

$$C_3F_6 \rightarrow CF_3 + C_2F_3 \qquad (6)$$

Because molecular beam techniques allow for the direct detection of the primary products in a unimolecular reaction, the present study using photofragment translational spectroscopy[13] coupled with IRMPD was undertaken.

In addition to the identification of the primary products, photofragment translational spectroscopy yields insight into the dissociation dynamics of a reaction through measurement of the translational energy release of the products. The observed translational energy distributions in hexafluoropropene decomposition may facilitate understanding of the CF_2 loss reaction. Although cleavage of a carbon−carbon double bond seems unusual, it is not unprecedented. In the 193 nm dissociation of tetrafluoroethylene, formation of two CF_2 fragments occurred via double-bond cleavage (7).[14]

$$C_2F_4 \rightarrow 2CF_2 \qquad (7)$$

In that case, a large translational energy release, peaked well away from zero, was observed as well as a polarization dependence, indicating dissociation from an excited state. It will be informative to compare the translational energy distributions and therefore the dynamics of these two systems, as the IRMPD of hexafluoropropene results in rupture of the double bond from the ground electronic state.

II. Experiment

These experiments were carried out at the Institute of Atomic and Molecular Sciences in Taiwan,[15] and the features of the rotating source molecular beam machine have been previously described.[16] Briefly, a mixture of 5% C_3F_6 in helium was passed through a solenoid-type pulsed valve (General Valve, Series 9) with a 0.020 in. nozzle, operating at room temperature with a typical stagnation pressure of 1 atm. The supersonic expansion of hexafluoropropene was characterized by standard time-of-flight techniques with a spinning slotted wheel, and a mean velocity of 900 m/s with a spread of ∼12% was found. The molecular beam was collimated with two skimmers, resulting in an angular divergence of slightly less than 3°. A Lambda Physik EMG 202 pulsed CO_2 laser was tuned to the P(26) line of the 9.6 μm branch (1041 cm^{-1}) and crossed the molecular beam at right angles in the interaction region. The laser beam was focused to a 1.5 × 2 mm^2 spot using a 1 in. ZnSe lens with a 25 cm focal length, resulting in a fluence of ∼10 J/cm^2. The fragments created by IRMPD traveled 36.7 cm to the detector that consisted of an electron impact ionizer, quadrupole mass filter, and Daly type ion detector.[17] A multichannel scaler triggered by the laser collected the ion counts as a function of the flight time from the interaction region to the detector.

III. Results and Analysis

Measurements were taken at source to detector angles of 15°, 20°, 30°, and 40° and laser-correlated dissociation signal was observed at *m*/*e* ratios 100 ($C_2F_4^+$ or $CFCF_3^+$), 81 ($C_2F_3^+$), 69 (CF_3^+), 62 ($C_2F_2^+$), 50 (CF_2^+), and 31 (CF^+). The signal at $m/e = 100$ is unambiguous evidence for the CF_2 loss channel. For the time being, this reaction will be referred to as reaction 1. As will be shown later, the laser-correlated signal at $m/e = 81$ is notably broader than that at $m/e = 100$, indicating the presence of a second primary channel (6). In addition, $m/e = 50$ shows evidence of a secondary dissociation channel.

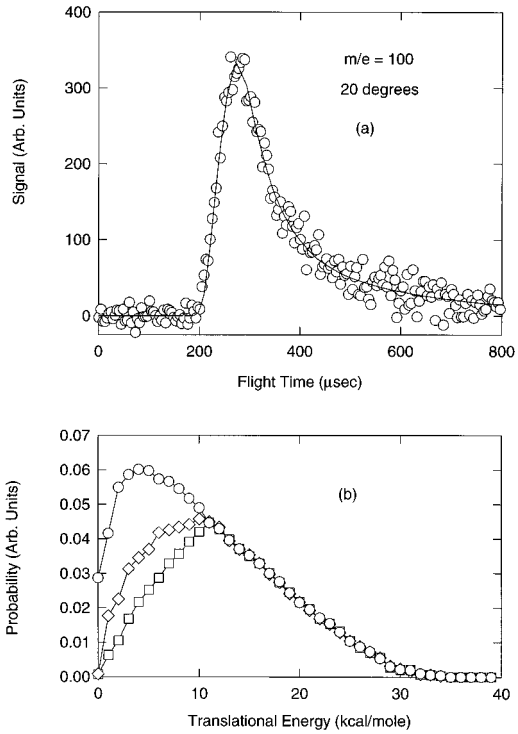

Figure 1. Experimental evidence for reaction 1. (a) Time-of-flight spectrum for $m/e = 100$ at 20°. The open circles represent data points, and the solid line is the fit to the data using the forward convolution method. (b) The center-of-mass translational energy distribution derived from $m/e = 100$ is represented by the open squares. Due to the secondary dissociation of $m/e = 100$, this distribution is biased toward molecules with greater translational energy. The open diamonds represent the translational energy distribution derived from the primary $m/e = 50$ fragment in Figure 4b, while the open circles are derived from Figure 4c. See text for details.

The resulting data were analyzed using standard forward convolution techniques.[18] A center-of-mass translational energy distribution is assumed for each channel, and the time-of-flight spectrum generated is averaged over apparatus functions, such as the ionizer width. This spectrum is then compared to the experimental time-of-flight spectrum, and the translational energy distribution is modified until the two match. In principle, for each dissociation channel it is necessary to measure only one of the dissociating fragments to obtain the center-of-mass translational energy. In practice, the time-of-flight spectra of all fragments are measured, and the conservation of linear momentum requirement in the center-of-mass system is used to ensure that the dissociation products are assigned to the correct channel.

A. Primary and Secondary Reactions. *1.* $C_3F_6 \rightarrow C_2F_4 + CF_2$. The time-of-flight spectrum of $m/e = 100$ is shown in Figure 1a. This confirms the unimolecular dissociation of hexafluoropropene by either reaction 1 or reaction 2 under collisionless conditions. The corresponding momentum matched partner, $m/e = 50$, will be discussed later. The translational energy distribution is derived from $m/e = 100$ time-of-flight spectra at 20°, 30°, and 40°. This distribution, which is peaked away from zero, is shown in Figure 1b. The average translational energy release is 13.3 kcal/mol.

2. $C_3F_6 \rightarrow CF_3 + C_2F_3$. As mentioned above, the signal observed at $m/e = 81$ ($C_2F_3^+$) could not be explained by assuming the only contribution was fragmentation of $m/e = 100$ in the electron impact ionizer. The discrepancy in the fit occurs at longer times, indicating the contribution of another channel with little translational energy. The differences between the

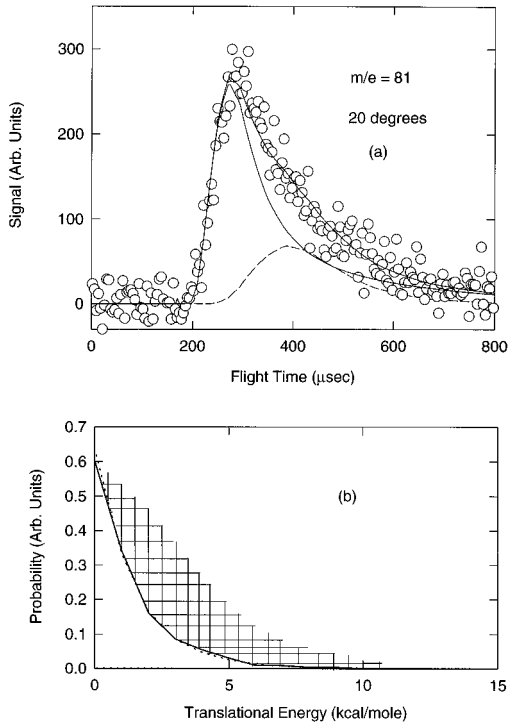

Figure 2. Evidence for the simple bond rupture reaction. (a) Time-of-flight spectrum for $m/e = 81$ at 20°. The solid line represents the $m/e = 100$ species that fragments in the ionizer to $C_2F_3^+$ while the dashed line represents the contribution of reaction 6 at $m/e = 81$. (b) The translational energy distribution of the products of reaction 6. The cross-hatched area represents the uncertainty associated with this measurement. The solid and dotted lines are the result of the IRMPD modeling calculations and are further explained in part B of section III.

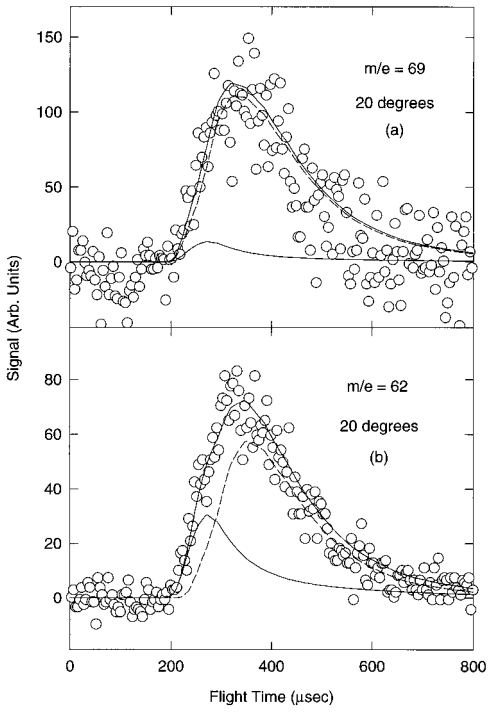

Figure 3. Time-of-flight spectra for $m/e = 69$ and 62 at 20°. (a) The trifluoromethyl fragment shows a large contribution from reaction 6 as indicated by the dashed line. It is the momentum matched partner of $m/e = 81$ shown in Figure 2a. A fast contribution, shown with the solid line, from the fragmentation of $m/e = 100$ in the electron impact ionizer is possible but not significant. (b) At $m/e = 62$ the dashed line indicates fragmentation from $m/e = 81$ while the solid line is fragmentation from $m/e = 100$. CFCF is not formed in any primary processes.

$m/e = 81$ and the $m/e = 100$ spectra can be explained by assuming a second primary channel involving CF_3 loss. The time-of-flight spectrum for $m/e = 81$ at 20° is shown in Figure 2a along with the corresponding translational energy distribution (Figure 2b). As expected, the translational energy distribution for the simple bond rupture reaction peaks near zero with a low average translational energy release. Further evidence of this slow channel is apparent in the time-of-flight spectra at $m/e = 69$, CF_3^+, and $m/e = 62$, $CFCF^+$ (Figure 3). The signal observed at these masses cannot be explained without considering reaction 6.

3. $C_2F_4/CF_3CF \rightarrow 2CF_2$. As fluorocarbons readily fragment in the electron impact ionizer, contributions from many higher molecular weight products are found in the lower m/e spectra. However, there is a portion of the $m/e = 50$ and 31 time-of-flight spectra that cannot be explained by the two primary reactions discussed above. Since the time-of-flight spectrum at $m/e = 31$ results solely from fragmentation of $m/e = 50$ giving no new information, we will focus on the $m/e = 50$ spectrum. In Figure 4a it is evident that the contributions from fragmentation of $m/e = 100$, 81, and 69 are not fast enough to fully explain the time-of-flight spectrum observed. CF_2 is also a primary product from reaction 1, and its contribution is illustrated in Figure 4a. It is constrained to be momentum matched to $m/e = 100$, and it is too fast to explain the additional signal observed. The secondary dissociation of the $m/e = 100$ species to form two CF_2 fragments seems to be the only viable explanation.

Determining the extent of secondary dissociation in hexafluoropropene is complicated by the overlapping signal of the primary and secondary reactions at $m/e = 50$. Fragment 4b illustrates one limiting case in which the secondary dissociaiton products have the minimum possible translational energy, while Figure 4c is a fit with faster secondary dissociation products. Figure 5 illustrates the range of these two secondary translational energy distributions. The distributions are both peaked away from zero, near 5 kcal/mol, while the average translational energy release ranges from 5.6 to 7.2 kcal/mol, respectively.

As a consequence of the secondary dissociation of the C_2F_4/CF_3CF species, the primary translational energy distribution for reaction 1 cannot be obtained from the $m/e = 100$ time-of-flight spectrum. The translational energy distribution derived from $m/e = 100$, shown in Figure 1b, is biased toward faster molecules with less internal energy since they do not undergo as much secondary decomposition. In other molecules, the primary translational energy distribution could be obtained by observing the corresponding momentum matched fragment. However, in hexafluoropropene the signal from CF_2 produced in the primary process cannot be separated from the secondary decomposition signal, which also results in CF_2. A comparison of the translational energy distributions obtained from the $m/e = 100$ time-of-flight spectrum (Figure 1a) and those obtained from the $m/e = 50$ primary dissociation signal (Figure 4b,c) is shown in Figure 1b. The difference between the $m/e = 100$ and 50 distributions was used as the primary translational energy distribution for the secondary dissociation products in both cases as previously discussed.[13a]

The method for calculating the experimental branching ratio between the two primary reactions has been discussed in detail earlier.[19] The branching ratio between reactions 1 and 6 was only determined at the maximum attainable fluence, ~10 J/cm^2, owing to limitations in detector sensitivity at lower fluences. The relative contribution from each primary fragment, C_2F_4, C_2F_3, CF_3 and CF_2, at each m/e ratio was determined. In the case of secondary dissociation, the contribution at $m/e = 50$ and 31 was included in the C_2F_4 yield, taking into account that each $m/e = 100$ fragment produces two CF_2 fragments. The

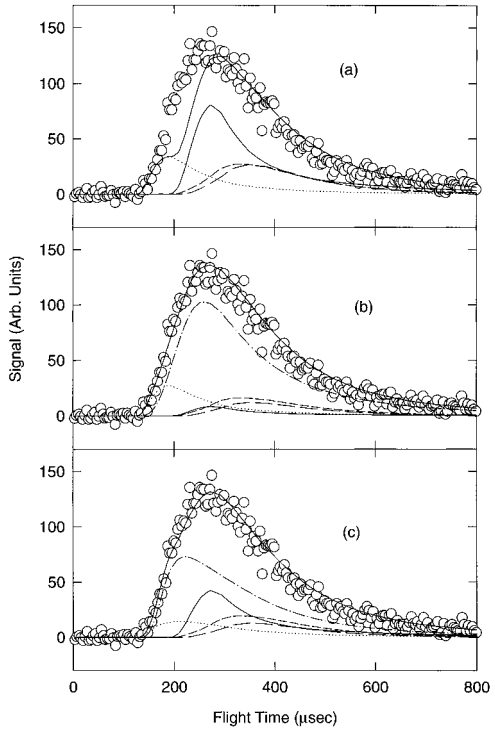

Figure 4. Time-of-flight spectra for $m/e = 50$ at 20°. (a) Contributions from $m/e = 100$ (solid line), $m/e = 81$ (long dashed line), $m/e = 69$ (short dashed line), and $m/e = 50$ (dotted line) cannot completely explain the signal observed at this mass. (b) The dash-dot-dash line represents the slowest possible contribution from secondary decomposition. The corresponding secondary translational energy distribution is shown in Figure 5. (c) In this representation the secondary dissociation (dash-dot-dash line) is as fast as possible while retaining a significant contribution of primary $m/e = 50$. The translational energy distribution in this case is also shown in Figure 5.

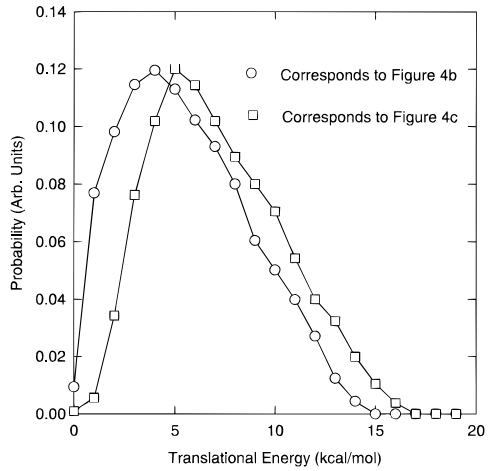

Figure 5. Limiting translational energy distributions for the secondary dissociation of $m/e = 100$. These distributions are derived from the dash-dot-dash lines in Figure 4b,c.

contributions of fragmentation at lower masses could not be quantified, which adds to the overall uncertainty. The branching ratio between reactions 1 and 6, $[CF_2]/[CF_3]$, was found to be 4.0 ± 1.0.

B. Using RRKM Theory To Obtain a Simple Bond Rupture Activation Energy. RRKM theory is often used to calculate dissociation rate constants for unimolecular reactions.[20] In the case of a simple bond rupture reaction without an exit barrier, one can predict the translational energy distribution based on the total available energy.[21] The resulting translational energy distribution is typically peaked at zero and decays exponentially. An extension of RRKM theory has been used in our group to calculate dissociation barriers in situations where a simple bond rupture and a concerted reaction compete.[13] In order to determine a dissociation barrier for reaction "A", it is necessary to know the activation energy for reaction "B", the experimental branching ratio, and the simple bond rupture translational energy distribution. A program that models the competition between absorption, stimulated emission, and dissociation is used to obtain the population created by the laser and the yield of each channel.[22] RRKM translational energy distributions at each energy level above dissociation are weighted by the population distribution of the excited parent and summed to create the overall translational energy distribution, which is compared to the experiment.[23] This iterative process entails modifying the quasi-continuum cross sections using different barrier heights until the experimental branching ratio and translational energy distribution are reproduced.

The dissociation rate constants and translational energy distributions for hexafluoropropene were determined using a readily available RRKM program.[24] The ground state vibrational frequencies necessary for the RRKM calculations were obtained from the literature.[9b] The transition state frequencies were assumed to be similar to the ground state and then varied to reproduce the preexponential A factor. For reaction 1 an A factor of 13.0 was utilized,[1,2] while for reaction 6 a typical A factor for fluorocarbons undergoing simple bond rupture of 16.1 was assumed.[25] Table 1 lists the relevant RRKM parameters. To predict the population created by infrared multiphonon excitation, a laser pulse consisting of a 100 ns spike followed by a 1 μs tail was used.[26] We assumed the spike contained 70% of the total available energy as has been reported for CO_2 laser pulses.[27]

Two values have been measured for the activation energy of reaction 1 (75[1,2] and 82.7[4] kcal/mol). In Figure 2b, the dotted line represents the best fit using an activation energy of 75 kcal/mol for reaction 1; a barrier height of 100 kcal/mol was obtained for reaction 6. The solid line represents a second calculation using 82.7 kcal/mol as the activation energy for CF_2 elimination. In this instance a barrier height of at least 105 kcal/mol is necessary to reproduce the experimental translational energy distribution. There is a large uncertainty in assigning an activation barrier to reaction 6 owing to the uncertainty in the value of the activation energy for reaction 1. In addition, the range of translational energy distributions that can be used to fit reaction 6 is large, as seen by the cross-hatched area in Figure 2b. At best, we can estimate that the barrier height for simple bond rupture of hexafluoropropene is 100−105 kcal/mol.

IV. Discussion

There is clear experimental evidence for reactions 1 and 6 as well as a secondary dissociation reaction in the IRMPD of hexafluoropropene. The formation of CF_3 from reaction 6 can explain the presence of C_2F_6 in earlier IRMPD studies[10−12] as recombination of the trifluoromethyl radicals is possible. The secondary dissociation reaction highlights the reactivity of C_3F_6, which may explain the extensive polymerization seen in previous experiments.[1,3,4,10−12] In the following paragraphs, we discuss possible reaction mechanisms for reaction 1 and the identity of the heavier species which undergoes secondary decomposition.

Difluorocarbene Loss. The mechanism by which CF_2 is formed in the dissociation of hexafluoropropene is not well understood. Although tetrafluoroethylene has been detected in a number of IRMPD and thermal experiments, there is still uncertainty as to whether it is formed in the primary decomposition step of hexafluoropropene. The adiabatic compression studies suggest that $CFCF_3$ is formed intially and then isomerizes to tetrafluoroethylene.[4] The consensus of the IRMPD studies

TABLE 1: Parameters Used in the RRKM Calculations

		vib freq (cm^{-1})		
			critical configuration[a]	
vib freq (cm^{-1})	description	molecule	CF_3 loss	CF_2 loss
1797	C═C stretch	1797	1797	**rxn coor**
1399	C−F stretch, CF_3	1399	1399	1399
1333	assym CF_2	1333	1333	1333
1211	C−F stretch, CF_3	1211	1211	1211
1179	C−F stretch, CF_3	1179	1179	1179
1122	C−F stretch	1122	1122	1122
1037	C−F stretch	1037	1037	1037
767	C−C stretch	767	**rxn coor**	767
655	CF_2 def	655	655	655
609	sym CF_3 def	609	**100**	609
559 × 2	asym CF_3 def	559 × 2	**100** × 2	559 × 2
513	CF_2 rock	513	513	513
462	CF_2 wag	462	462	462
370	CF wag	370	370	370
364	C−C−C def	364	**100**	364
250 × 2	C−F rock	250 × 2	250 × 2	250 × 2
171	CF_2 twist	171	171	**700**
134	CF_3 twist	not used	not used	not used
94	CF_3 rock	94	94	94
reduced moment of inertia for internal rotations (amu Å^2)[b]		79	79	79
external moments of inertia (amu Å^2)[c]			198, 403, 512	
energy threshold (kcal/mol)			varied	75, 82.7
calculated value log *A*			16.1	13.0

[a] The transition state frequencies in bold were modified to reproduce the preexponential *A* factor. [b] The CF_3 twist was treated as an internal rotation. See, for example: Gordy, W.; Cook, R. L. *Microwave Molecular Spectra*, 3rd ed.; Wiley: New York, 1984; p 574. [c] The external rotations were obtained from the rotational constants in: Jacob, E. J.; Lide, D. R. *J. Chem. Phys.* **1973**, *59*, 5877.

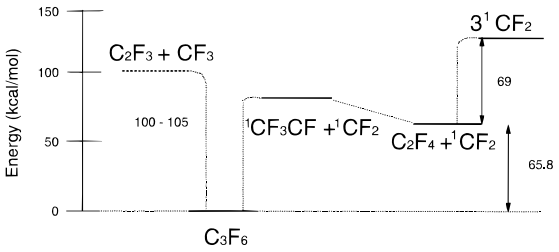

Figure 6. Energy level diagram for hexafluoropropene illustrating the observed dissociation pathways. The heats of formation at 298 K were obtained from the following sources: C_3F_6, −268.9 ± 2 kcal/mol, ref 29; C_2F_4, −157.4 ± .7 kcal/mol, *J. Phys. Chem. Ref. Data* **1985**, *14*, (Suppl. 1), 655; $CFCF_3$, −140.4 ± 2 kcal/mol, ref 4; $^1CF_2$, −44.2 ± 1 kcal/mol, ref 29. The dashed line illustrates the three competing pathways. No barrier in the formation of C_2F_4 from $CFCF_3$ is shown as suggested from ref 4. The activation energy for reaction 6, CF_3 + C_2F_3, is an estimate from IRMPD modeling.

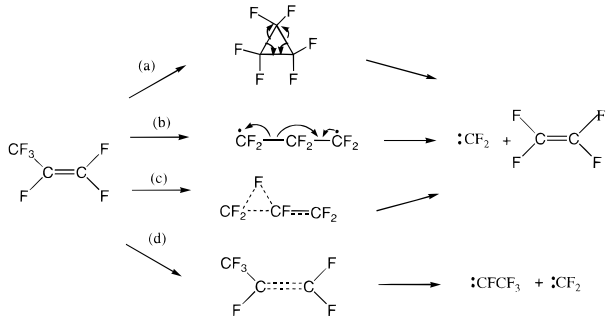

Figure 7. Four dissociation mechanisms for the elimination of CF_2 are illustrated: (a) isomerization to hexafluorocyclopropane occurs prior to dissociation; (b) a diradical, $CF_2CF_2CF_2$, is formed by fluorine migration; (c) a concerted mechanism in which fluorine migration and tetrafluoroethylene formation occur simultaneously; (d) direct cleavage of the double bond occurs as the carbon−carbon double bond elongates.

is that tetrafluoroethylene is generated directly from hexafluoropropene; however, no mechanism is given.[10−12] Benson suggests that an intermediate, cyclohexafluoropropane, proceeds tetrafluoroethylene formation.[2] Another intermediate that could be involved is the diradical $CF_2CF_2CF_2$; the presence of its hydrocarbon analog, trimethylene, has been predicted in the isomerization from cyclopropane to propene.[28]

By examining the possible dissociation pathways and the reaction dynamics, it may be possible to eliminate some mechanisms based on the observed translational energy distribution. The formation of the cyclic isomer, cyclohexafluoropropane, is energetically possible as it lies only 35.1 kcal/mol above the ground state of hexafluoropropene.[29] Direct dissociation of cyclohexafluoropropane should result in the expulsion of CF_2 as two single bonds are broken while a double-bond closed-shell species (tetrafluoroethylene) is formed (Figure 7a). This repulsion would result in a translational energy distribution peaked away from zero. If dissociation occurred from the diradical species, $CF_2CF_2CF_2$, the transition state might be expected to look like that of a simple bond rupture with one of the carbon−carbon single bonds stretching until two distinct species are formed (Figure 7b). Although some electronic rearrangement would be necessary to form tetrafluoroethylene, the translational energy distribution should peak at or near zero. An important caveat is that the $CF_2CF_2CF_2$ diradical may not be a distinct transition state; a concerted mechanism whereby a fluorine migrates as tetrafluoroethylene forms is plausible (Figure 7c). This concerted reaction might be expected to have an exit barrier which would result in a translational energy distribution peaked away from zero. On the other hand, if the products CF_2 and $CFCF_3$ are formed, they could result from direct cleavage of the carbon−carbon double bond (Figure 7d). One might initially think that the stretching of this bond to form two carbenes would result in a translational energy distribution similar to that for a simple bond rupture reaction. However, if we assume that C_3F_6 behaves in a manner similar to C_2F_4, the application of the Woodward−Hoffman rules predicts a barrier to the formation of the parent from two singlet species.[30] The unusual stability of singlet CF_2, owing to the large electronegativity and lone pairs on the fluorine atom,[31] results in a singlet−

triplet splitting of 56.6 kcal/mol.[32] On the other hand, the singlet−triplet splitting for $CFCF_3$ has been calculated to be only 9.2 kcal/mol.[33] These ground state singlet species, CF_2 and $CFCF_3$, have no open-shell electrons and therefore require energy for the excitation of each species in order to form covalent bonds.[31] The energy released from electron pairing to form the two singlet species in the reverse reaction of C_3F_6 dissociation would result in a translational energy distribution peaked away from zero.

The range of the primary translational energy distribution for the formation of CF_2 and its momentum matched partner is represnted in Figure 1b. The uncertainty in this distribution, as discussed earlier, lies in our inability to separate CF_2 formed in the primary step from that produced in the secondary dissociation reaction. This distribution does peak away from zero to a maximum of 10 kcal/mol and extends to 30 kcal/mol, which eliminates the involvement of the diradical (Figure 7b) as an intermediate. The isomerization of hexafluoropropene to perfluorocyclopropane, the concerted fluorine migration, or cleavage of the double bond could all result in the observed primary translational energy distribution. Although the barrier from hexafluoropropene to perfluorocyclopropane is estimated to be greater than 90 kcal/mol,[34] the IRMPD/RRKM calculations suggest that the excited fluorocarbon contains at least 100−105 kcal/mol, which may be enough for this isomerization to take place.

The possibility of isomerizations (Figure 7a) or fluorine migrations (Figure 7c) cannot be definitively ruled out in the IRMPD of hexafluoropropene. In both the IRMPD of hexafluoropropene and the UV photolysis of tetrafluoroethylene,[14] the translational energy distributions peak away from zero in the reaction which destroys the double bond, but the dynamics are not similar. In the case of tetrafluoroethylene photodissociation at 193 nm, the cleavage of the carbon−carbon double bond occurs on a short (picosecond) time scale as indicated by the slight polarization dependence ($\beta = -0.2$). In the IRMPD of hexafluoropropene, where the dissociation occurs on the nanosecond or longer time scale, it is unclear whether direct cleavage of the double bond is the mechanism that takes place.

Secondary Dissociation. The primary product, $CFCF_3$ or C_2F_4, undergoes further dissociation to produce two difluorocarbene species. The translational energy distribution from the secondary dissociation of hexafluoropropene (Figure 5) peaks near 5 kcal/mol and extends to ∼16 kcal/mol. A similar translational energy distribution is observed in the IRMPD of 2-chloro-1,1,1,2-tetrafluoroethane.[35] The complementary fragment in the elimination of HCl is CF_3CF, and the secondary dissociation of this fragment results in a translational energy distribution peaked at 3 kcal/mol and extending to ∼20 kcal/mol. These two very similar distributions indicate that the same dissociation mechanisms occur in both hexafluoropropene and 2-chloro-1,1,1,2-tetrafluoroethane. One pathway, suggested by Yokoyama and co-workers, is that trifluoromethylfluorocarbene directly undergoes a three-centered concerted dissociation reaction to form two CF_2 carbenes. This is the reverse reaction of CF_2 insertion into the CF bond of CF_2, and typically insertion reactions of carbenes with singlet ground states such as CF_2 will have barriers.[36] This entrance barrier translates into an exit barrier for $CFCF_3$ dissociation and will lead to a translational energy distribution peaked away from zero as observed.

A 1,2-fluorine atom shift to tetrafluoroethylene followed by dissociation could also produce the CF_2 observed in the secondary dissociation of hexafluoropropene and 2-chloro-1,1,1,2-tetrafluoroethane. In the analogous hydrocarbon system, $^1CH_3CH$ is predicted to have only a 0.6 kcal/mol barrier to the formation of ethylene via a 1,2 H shift.[37] In general, the activation energy for a 1,2 shifts increases in the following manner: Cl < H < alkyl < F.[7] Although calculations[8] and experiments[7] on $^1CF_3CH$ indicate a barrier greater than 20 kcal/mol for fluorine migration, it could occur as suggested by Buravtsev et al.[4] As discussed earlier, the formation of two singlet species in the cleavage of a double bond is likely to result in a translational energy distribution peaked away from zero. Preliminary results from the IRMPD of octafluorocyclobutane show that the C_2F_4 produced in the primary reaction dissociates further to CF_2.[38] The translational energy distribution for CF_2 formation is peaked away from zero at ∼4.5 kcal/mol and extends to 20 kcal/mol, which is similar to both our experiment and that of Yokoyama and co-workers. Although the same species appears to be undergoing secondary dissociation in all three experiments, it remains unknown whether dissociation occurs from C_2F_4, $CFCF_3$, or an intermediate species. It is not possible in this situation to determine the identity of the dissociation product based solely on the observed translational energy distribution.

V. Conclusion

Two primary pathways, CF_3 loss and CF_2 loss, have been observed in the IRMPD of hexafluoropropene. The loss of CF_3 has not been previously observed in the unimolecular decomposition of this molecule and may explain the observation of C_2F_6 in bulk experiments. Modeling the dissociation with a well-known RRKM/IRMPD model gives an activation energy of 100−105 kcal/mol for this simple bond rupture reaction. CF_2 loss was seen to be the predominant channel, accounting for 80% of the products, with significant secondary dissociation of the heavier fragment producing additional CF_2.

Acknowledgment. C.A.L. thanks Dr. T. T. Miau and Dr. A. G. Suits for many helpful discussions. The hexafluoropropene was kindly supplied by Dr. M. H. Hung at Du Pont. This work was supported by the Director, Office of Energy Research, Office of Basic Energy Sciences, Chemical Sciences Division of the U.S. Department of Energy, under Contract DE-AC03-76SF00098. Additional funding for this project was provided by Du Pont.

References and Notes

(1) Atkinson, B.; Trenwith, A. B. *J. Chem. Soc.* **1957**, 2082.
(2) Benson, S. W.; O'Neal, H. E. *Kinetic Data on Gas Phase Unimolecular Reactions*; National Bureau of Standards, U.S. Government Printing Office: Washington, DC 1970; p 493.
(3) Matula, R. A. *J. Phys. Chem.* **1968**, *72*, 3054.
(4) Buravtsev, N. N.; Grigor'ev, A. S.; Kolbanovskii, Y. A. *Kinet. Catal.* **1989**, *30*, 13.
(5) Heicklen, J.; Knight, V. *J. Phys. Chem.* **1965**, *69*, 3600.
(6) Dalby, F. W. *J. Chem. Phys.* **1964**, *41*, 2297.
(7) Holmes, B. E.; Rakestraw, D. J. *J. Phys. Chem.* **1992**, *96*, 2210.
(8) So, S. P. *J. Phys. Chem.* **1993**, *97*, 11908.
(9) (a) Edgell, W. F. *J. Am. Chem. Soc.* **1948**, *70*, 2816. (b) Nielsen, J. R.; Classen, H. H.; Smith, D. C. *J. Chem. Phys.* **1952**, *20*, 1916.
(10) Nip, W. S.; Drouin, M.; Hackett, P. A.; Willis, C. *J. Phys. Chem.* **1980**, *84*, 932.
(11) Santos, M.; Siguenza, C.; Torresano, J. A.; Gonzalez-Diaz, P. F. *Spectrochim. Acta* **1990**, *46A*, 455. Siguenza, C.; Santos, M.; Torresano, J. A.; Pino, A.; Gonzalez-Diaz, P. F. *Spectrochim. Acta* **1990**, *46A*, 1499.
(12) Torresano, J. A.; Santos, M.; Gonzalez-Diaz, P. F. *Laser Chem.* **1994**, *14*, 217.
(13) (a) Hintsa, E. J.; Wodtke, A. M.; Lee, Y. T. *J. Phys. Chem.* **1988**, *92*, 5379. (b) Wodtke, A. M.; Hintsa, E. J.; Lee, Y. T. *J. Phys. Chem.* **1986**, *90*, 3549. (c) Wodtke, A. M.; Lee, Y. T. In *Advances in Gas Phase Photochemistry and Kinetics*; Ashfold, M. N. R., Baggot, J. E., Eds.; Royal Society of Chemistry: London, 1987.
(14) Minton, T. K.; Felder, P.; Scales, R. C.; Huber, J. R. *Chem. Phys. Lett.* **1989**, *164*, 113.
(15) Lee, Y. R.; Chen, F. T.; Hsueh, C. C.; Chou, H. M.; Chen, H. C.; Yang, Y. J.; Lin, S. M. *Proc. Natl. Sci. Counc., Repub. China, Part A* **1994**, *18*, 55.
(16) Wodtke, A. M.; Lee, Y. T. *J. Phys. Chem.* **1985**, *89*, 4744.

(17) Lee, Y. T.; McDonald, J. D.; LeBreton, P. R.; Herschbach, D. R. *Rev. Sci. Instrum.* **1969**, *40*, 1402.

(18) Wodtke, A. M. Ph.D. Thesis, University of California at Berkeley, 1986. Zhao, X. Ph.D. Thesis, University of California at Berkeley, 1988.

(19) Myers, J. D. Ph.D. Thesis, University of California at Berkeley, 1993.

(20) Robinson, P. J.; Holbrook, K. A. *Unimolecular Reactions*; Wiley: London, 1972. Forst, W. *Theory of Unimolecular Reactions*; Academic Press: New York, 1973.

(21) Safron, S. A.; Weinstein, N. D.; Herschbach, D. R.; Tully, J. C. *Chem. Phys. Lett.* **1972**, *12*, 564.

(22) This program was first reported by: Schulz, P. A.; Sudbo, As. S.; Grant, E. R.; Shen, Y. R.; Lee, Y. T. *J. Chem. Phys.* **1980**, *72*, 4495.

(23) Butler, L. J.; Buss, R. J.; Brudzynski, R. J.; Lee, Y. T. *J. Phys. Chem.* **1983**, *87*, 5106.

(24) Hase, W. L.; Bunker, D. L. Quantum Chemistry Program Exchange, Indiana University, Prog. QCPE 234.

(25) Tschuikow-Roux, E. *J. Chem. Phys.* **1965**, *43*, 2251. Kato, S.; Makide, Y.; Tominaga, T.; Takeuchi, K. *J. Phys. Chem.* **1987**, *91*, 4278.

(26) Chowdhury, P. K.; Rama Rao, D. V. S.; Mittal, J. P. *J. Phys. Chem.* **1988**, *92*, 102.

(27) Grimley, A. J.; Stephenson, J. C. *J. Chem. Phys.* **1981**, *74*, 447. Stephenson, J. C.; King, D. S. *J. Chem. Phys.* **1978**, *69*, 1485. Beaulieu, J. A. *Proc. IEEE* **1971**, *59*, 667.

(28) Bergmen, R. J. In *Free Radicals*; Kochi, J. K., Ed.; Wiley: New York, 1973; Vol. 1, Chapter 5.

(29) Bomse, D. S.; Berman, D. W.; Beauchamp, J. L. *J. Am. Chem. Soc.* **1981**, *103*, 3967.

(30) The orbital and state correlation diagrams for the formation of C_2F_4 from two singlet species can be drawn and indicate a barrier exists between reactants and products. Woodward, R. B.; Hoffmann, R. *The Conservation of Orbital Symmetry*; Academic Press: New York, 1970. Atkins, P. W. *Molecular Quantum Mechanics*, 2nd ed.; Oxford University Press: New York, 1983; pp 336−345.

(31) Carter, E. A.; Goddard, W. A. *J. Phys. Chem.* **1986**, *90*, 998.

(32) Koda, S. *Chem. Phys. Lett.* **1978**, *55*, 353; *Chem. Phys.* **1982**, *66*, 383.

(33) Dixon, D. A. *J. Phys. Chem.* **1986**, *90*, 54.

(34) Berman, D. W.; Bomse, D. S.; Beauchamp, J. L. *Int. J. Mass Spectrom. Ion Phys.* **1981**, *39*, 263.

(35) Yokoyama, A.; Yokoyama, K.; Fujisawa, G. *J. Chem. Phys.* **1994**, *100*, 6487.

(36) Bach, R. D.; Su, M.-D.; Aldabbagh, E.; Andres, J. L.; Schlegel, H. B. *J. Am. Chem. Soc.* **1993**, *115*, 10237. Haszeldine, R. N.; Parkinson, C.; Robinson, P. J.; Williams, W. J. *J. Chem. Soc., Perkin Trans. 2* **1979**, 954.

(37) Evanseck, K. D.; Houk, K. N. *J. Phys. Chem.* **1990**, *94*, 5518.

(38) Lee, Y. R.; Lin, S. M. To be published.